Journal of Power Sources 202 (2012) 100–107

Contents lists available at SciVerse ScienceDirect

Journal of Power Sources

journal homepage: www.elsevier.com/locate/jpowsour

Effect of GDL deformation on the pressure drop of polymer electrolyte fuel cell separator channel

Litan Kumar Saha[a,*], Yutaka Tabe[b], Nobuyuki Oshima[b]

[a] Department of Mathematics, University of Dhaka, Dhaka 1000, Bangladesh
[b] Graduate School of Engineering, Hokkaido University, Sapporo, 060-8628, Japan

ARTICLE INFO

Article history:
Received 6 August 2011
Received in revised form 6 November 2011
Accepted 15 November 2011
Available online 23 November 2011

Keywords:
Gas diffusion layer
Pressure drop
Deformation thickness
Separator channel
Numerical simulation

ABSTRACT

In this study the deformation effect of a gas diffusion layer (GDL) on the pressure drop of a polymer electrolyte fuel cell (PEFC) separator channel has been investigated both numerically and experimentally. Pressure drop is considered as a diagnostic tool to monitor the performance of a PEFC. The deformation of the GDL caused by the compression pressure plays an important role in the performance of a PEFC since it affects the physical properties of the GDL, such as porosity, permeability and the cross sectional area of the gas channel. The flow behavior in the separator channel and GDL of PEFCs has been investigated by using a transient, isothermal and three-dimensional numerical model. To develop the numerical simulation of PEFC, verification experiments and data acquisition of physical parameters were conducted by mechanical measurements. The experimental results showed that estimating the actual flow configuration in the cell, the GDL deformation shape due to clamping by the separator lands has a significant influence. The numerical result shows that together with the deformation shape, the GDL physical parameter variation also needs to be considered in order to predict the actual flow phenomena. Moreover, the results can estimate the physical parameters under deformed condition qualitatively.

1. Introduction

The working formula of an electrochemical fuel cell is to convert the chemical energy of hydrogenised fuel directly into electrical energy. Fuel cells are classified depending upon the nature of the electrolyte used in the system. Polymer electrolyte fuel cells (PEFCs) are considered as prime candidates among the fuel cells under development because of their high power density, low operating temperature, low emissions and environmental friendly nature. This recognizes PEFC as a suitable alternative power source for next-generation vehicles and portable power plants. In order to achieve large-scale market penetration, the performance of PEFCs must be improved.

Operating parameters such as pressure, temperature and flow distribution in the flow channel and GDL have a great influence on the performance of polymer electrolyte fuel cells. A certain pressure drop is beneficial for fuel cell operation because it helps to remove excess liquid water from the cell, though too much pressure drop would increase the parasitic power needed to pump air through the fuel cell [1]. It is desired to have an optimum pressure drop in the separator channel because too large pressure drop leads to inefficient fuel cell performance. The effects of different operating parameters on the performance of proton exchange membrane (PEM) fuel cells have been studied experimentally by Wang et al. [2]. Hydrogen is used as the fuel on the anode side whereas oxygen is used as the fuel on the cathode side; the cell produces water and heat as by-products. Since both the reactants and the byproduct pass through the channel and GDL are considered important parts of a PEFC.

The design of the flow channels and bipolar plates is critical for the performance of the resulting PEFCs [3–7]. A methodology for designing the flow channels for PEFCs, including channel layout, configuration, channel cross-section and channel length was developed by Li et al. [3]. Barbir et al. [1] investigated the relationship between pressure drop and cell resistance as a diagnostic tool for PEFCs. They observed that an increase in pressure drop is a reliable indicator of polymer electrolyte fuel cell flooding. By monitoring both the pressure drop and cell resistance they were able to diagnose either flooding or drying. He et al. [8] investigated the pressure drop between inlet and outlet channels as a diagnostic tool to monitor liquid water flooding. Cross-leakage flow through the electrode has been investigated as a direct result of the pressure difference between the adjacent flow channels of PEM fuel cells by Kanezaki et al. [9] and Park and Li [10].

The gas diffusion layer in a polymer electrolyte fuel cell consists of a thin layer of carbon black mixed with polytetrafluoroethylene (PTFE) [11] that is coated on a sheet of macro-porous carbon backing cloth. The GDL permits the gaseous reactants to move towards

* Corresponding author. Tel.: +880 1715765533.
E-mail address: lksaha_math@yahoo.com (L.K. Saha).

0378-7753/$ – see front matter © 2011 Elsevier B.V. All rights reserved.
doi:10.1016/j.jpowsour.2011.11.038

Nomenclature

a	height of the channel, m
A	area, m^{-2}
b	width of the channel, m
d	deformation thickness, m
K	permeability, m^2
L	length of the flow channel, m
p	pressure, Pa
Q	volume Flow rate, $m^3 s^{-1}$
t	time, s
$\boldsymbol{u}$	flow velocity in the flow channel, ms^{-1}
u	velocity in the x direction, ms^{-1}
v	velocity in the y direction, ms^{-1}
w	velocity in the z direction ms^{-1}

Greek symbols

ε	porosity of porous media
μ	viscosity, $kg\,m^{-1}\,s^{-1}$
ρ	density, $kg\,m^{-3}$

the catalyst layer and maintains the flow of electrons between catalyst layers and bipolar plates. The diffusion layer also plays a critical role in water management within the cell. It provides a physical micro-porous support for the catalyst layer. The GDL is a porous material, and the flow distribution inside the porous media is very complex. The effect of the diffusion layer parameter on the performance of PEFC [12–16] has received a great deal of attention.

The gas diffusion layers and bipolar plates are usually clamped together under suitable pressure in order to seal the fuel cell against any gas leakage and to minimize the contact resistance between the rib and the GDL. The influence of the clamping force on the performance of a polymer electrolyte fuel cell with interdigitated gas distribution was investigated by Zhou et al. [17,18] whereas in a more recent work by Zhou et al. [19] the conventional flow field was considered. They found that the clamping force affects the permeability and diffusion of the reactant gas transport of the liquid water due to GDL deformation and porosity variation. Chang et al. [20] found experimentally that the external clamping pressure changes not only the thickness but also the porosity and permeability of the GDL. Roshandel et al. [21] and Roshandel and Farhanieh [22] examined the variation of porosity distribution considering both the effect of the compression of the electrodes on the solid landing area and the water generated at the cathode side of GDL. Gurau et al. [23] derived an analytical solution of a half-cell model for the polymer electrolyte membrane fuel cell considering the non-uniform porosity of the gas diffusion layer. Nitta et al. [24] experimentally investigated the effect of inhomogeneous compression of the GDL caused by the channel/rib structure of the flow field plate. They observed that the GDL under the channel remained at almost the initial thickness regardless of the width of the channel. On the other hand the GDL under the bipolar plate was compressed to gasket thickness. Basu et al. [25] found that the high compression pressure pushes the softer GDL material into the channel, partially blocking the channels. The compression pressure is the highest at the edge (near the location of the tightening bolts), so GDL intrusion is most severe at the edge channels. They used an experimental pressure drop to match the deformation level but the variation of physical parameters was not studied. None has reported dependence of the pressure drop on the clamping pressure. In this study a detailed investigation of the pressure drop in various deformation cases and various physical conditions has been carried out.

The objective of the present work was to study the influence of GDL properties on the pressure drop in the separator channel. The influence of the key parameters and its effect in the uncompressed and compressed conditions were studied, and the pressure loss mechanism in the compressed PEFC condition was identified. Also, the effect of GDL deformation on the physical property of the diffusion layer will be analyzed qualitatively.

2. Experimental setup and methods

Fig. 1 provides experimental fuel cell and a schematic view of the single PEFC used in this study. PEFCs use a polymeric membrane as an electrolyte, such as Nafion 117 polymer, which is sandwiched between two electrodes, namely the anode and cathode. The interface between the electrode and the polymeric membrane is the catalyst layer, and it has a reaction area of $3 \times 10\,cm^2$. A separator with straight parallel gas flow channel, as shown in Fig. 1(b), was used on both the anode and the cathode side of PEFC. The width of the channels and the ribs of both separators were 1 mm. The thickness of the separator, which corresponds to the channel height, was 0.5 mm. Carbon paper with a thickness of 0.3 mm was used for the GDL, and the cell was bolted together uniformly by different clamping pressure. The pressure drop from the channel inlet to channel outlet was measured using a digital manometer for two different conditions: with and without the GDL. For the latter case, a plastic wall was used instead of a GDL. Performance analysis was conducted under several driving conditions. GDL deformations due to the clamping pressure of the separators and the pressure drop of the cathode gas channel were measured under various deformation conditions. The deformation shape of the GDL was visualized using a section-observable separator, and an image was recorded by a digital camera after applying the compression pressure.

3. Numerical methods

3.1. Model formulations

The gas flow channels are typically rectangular or square grooves machined on the separator plate that distribute reactant gas over the fuel cell. A conventional separator plate with straight parallel gas channel is considered in this study. The flow configuration in the parallel channel layout is symmetrical. To reduce the computational effort, symmetry consideration is assumed and only one gas channel with the half of the rib region on both sides of the channel, highlighted by the dotted line in Fig. 1(b), is considered in the present numerical investigation. We wanted to focus our investigation on the physical properties of the GDL that can be deduced by observing the flow behavior inside this channel and GDL. The dimensions of the gas channel, separator and GDL used to conduct the simulation are listed in Table 1. For simplification, the following assumptions were made: (1) an ideal gas mixture; (2) incompressible and laminar flow due to a small Reynolds number; (3) an isotropic porous media for the GDL. Here we investigated the gas flow only. Electric current and liquid water were not studied in this paper. The same code was used to consider the electric current and liquid water by Shi et al. [26,27]. Deformation of the GDL was considered in our present investigation. The numerical grid and its distribution pattern are shown is Fig. 2.

Table 1
Dimension of the computational domain for different deformation shapes.

	Thickness of GDL under bipolar plate (m)
Without deformation	3.0×10^{-4}
Deformation 1	2.0×10^{-4}
Deformation 2	1.75×10^{-4}
Deformation 3	1.6×10^{-4}

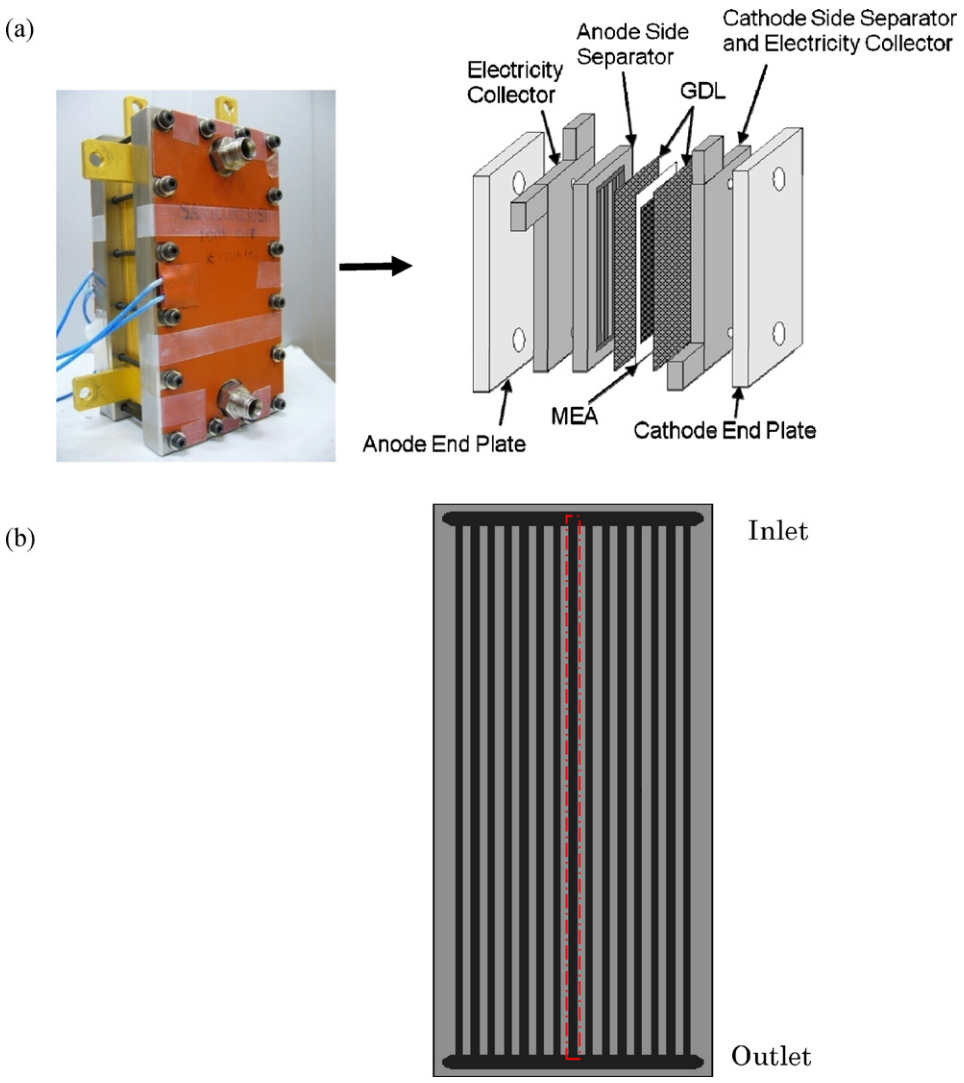

Fig. 1. (a) Experimental fuel cell and schematic view of full PEFC model and (b) typical cross section of separator channel.

Experimental observation of the GDL shape before and after application of the compression pressure is shown in Fig. 3. From this figure we see that the deformation shape of the GDL is non-uniform. We also observe that deformation of GDL under the separator is highly compressed but less compressed under the channel region. Moreover, under the center of the channel it remains unaltered. Before applying compression force the thickness of the GDL was 0.3 mm. The deformation of the GDL depends upon the compression pressure applied on it. Three different levels of deformation were chosen as shown in Fig. 8 in the results and discussion section. The computational grid used for the present simulation has nearly the same deformation shape as in the experimental data.

3.2. Governing equations

The flow field in the separator channel and GDL can be obtained by solving the conservation equations of mass and momentum. A single set of governing equations valid for the sub regions (1) gas channel and (2) porous GDL is used. Therefore, interfacial conditions of the internal boundaries between gas channel and GDL need not to be specified. Considering the assumptions the governing equations can be written as:

Mass conservation:

$$\frac{\partial(\varepsilon\rho)}{\partial t} + \nabla\cdot(\varepsilon\rho\boldsymbol{u}) = 0 \tag{1}$$

Momentum conservation:

$$\frac{\partial\varepsilon\rho\boldsymbol{u}}{\partial t} + \nabla\cdot(\varepsilon\rho\boldsymbol{u}\boldsymbol{u}) = -\nabla(\varepsilon p) + \nabla\cdot(\varepsilon\mu\nabla\boldsymbol{u}) + \varepsilon\rho g - \frac{\mu}{K}\varepsilon^2\boldsymbol{u} \tag{2}$$

where $\boldsymbol{u}$ is the velocity vector, μ the viscosity, ρ the density, ε the porosity of the GDL and K is the permeability of the GDL. Porosity, ε is defined by the ratio of the volume occupied by the pore to the total volume of the porous media where as permeability, K is defined by the square of the effective volume to surface area ratio of the porous matrix [28]. The last term of Eq. (2) represents the Darcy's drag force in the porous media. In the gas channel, $\varepsilon \to 1$ and $K \to \infty$, so Eq. (2) becomes the original Navier–Stokes equation.

3.3. Boundary conditions

A constant velocity was applied to the inlet boundary of the channel. All wall boundary conditions were considered as no-slip. A constant pressure condition was used at the outlet of the flow channel.

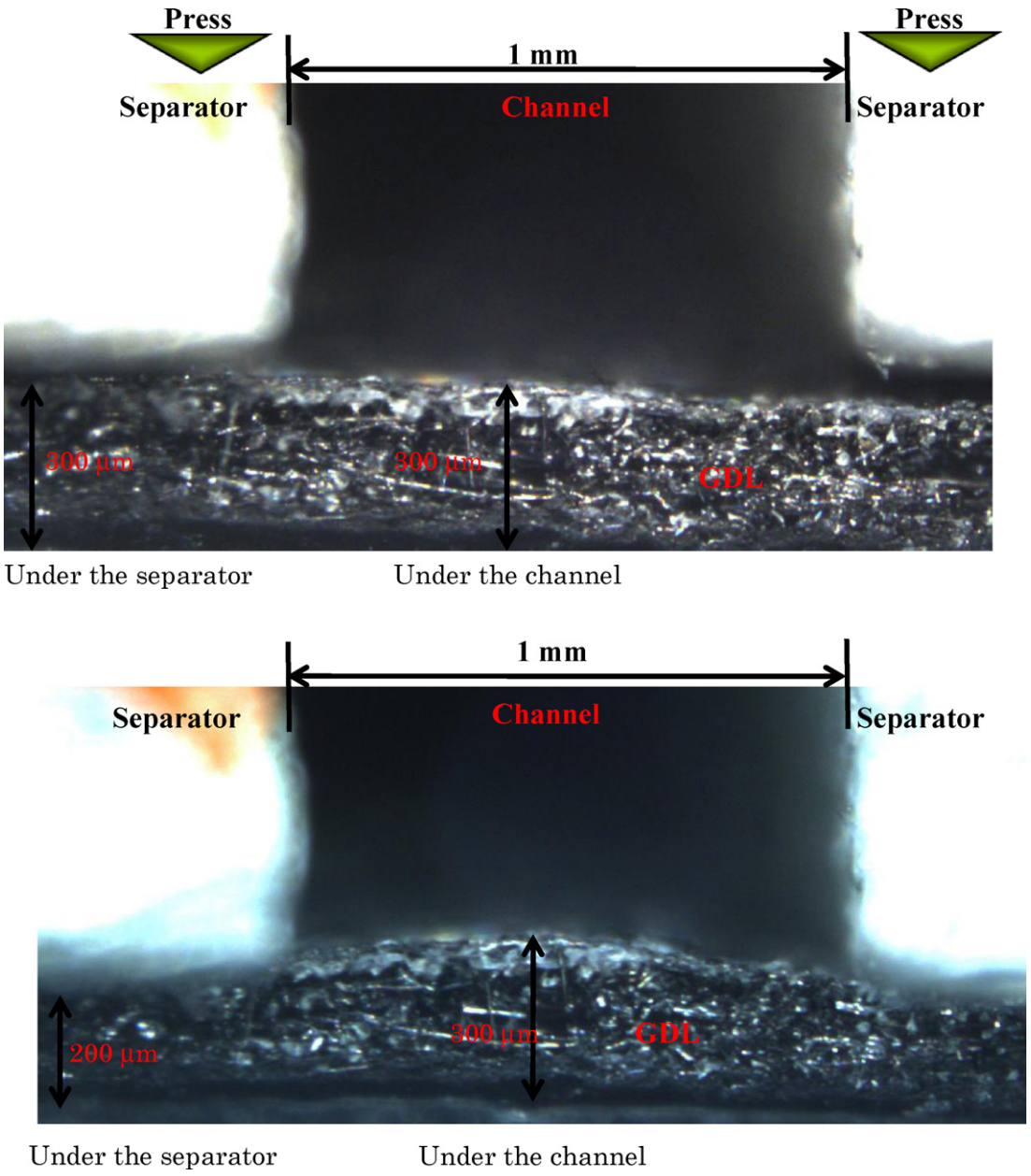

Fig. 2. Computational grid for the deformation of GDL.

3.4. Numerical method

The conservation equations of mass and momentum, together with the boundary condition, are discretized by the finite volume method and solved by the software ForntFlow/PEFC, which is a general purpose numerical simulator. The numerical simulator, developed by the Computational Fluid Mechanics laboratory of Hokkaido University and supported by New Energy and Industrial Technology Development Organization (NEDO), also includes an electrical field, porous media, electrochemical reaction and water transport. The flow behavior inside the porous media will be treated as a key technology for this flow simulator. The implicit Euler scheme was used for time integration. The first order upwind scheme was applied to discretize the convection terms in the governing equations. The fractional step algorithm was used to update the pressure and velocity fields from the solutions of the pressure Poisson equation. Implicit treatment of the Darcy drag term was considered to get an accurate continuity condition and precise estimation of pressure loss. Details of the algorithm and the advantage of using the algorithm have been reported by Saha et al. [29]. The solutions are considered to be convergent if the variables of Eqs. (1) and (2) have an absolute error less than 10^{-8} and a relative maximum error less than 10^{-6}. The computational grid system of the present model consists of 0.26 million grid points. The time required for each case on an AMD Opteron 3.2 GHz system with 2 GB of main memory was around 12 h.

4. Pressure drop in the gas flow channel

The pressure drop is a result of frictional loss and bending loss in the gas flow channel. In a straight channel, the loss coefficient can be approximated only by the friction loss coefficient. The pressure

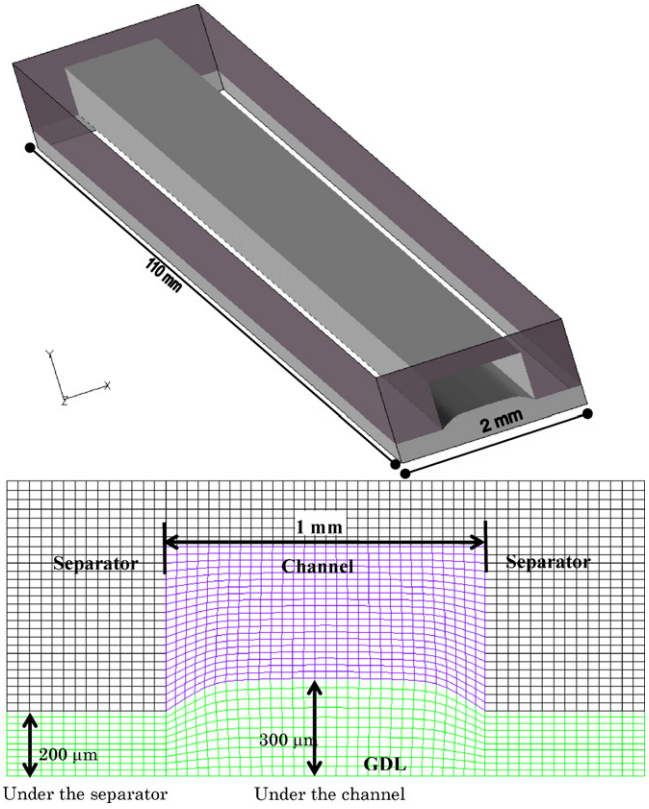

Fig. 3. GDL deformation before (upper) and after (below) applying the compression pressure.

drop between the inlet and outlet of a rectangular channel can be calculated using Darcy's law for uniform, non-compressible pipe flow:

$$\Delta p = f\frac{L}{d_h}\frac{\rho V^2}{2} \tag{3}$$

where f is the friction factor, L the length of the channel, ρ the density of the fluid, V the average velocity of the fluid, equal to the volumetric flow rate per unit cross-sectional area, and d_h the hydraulic diameter of the flow path, which can be defined as:

$$d_h = \frac{4ab}{2(a+b)} \tag{4}$$

where a and b are the sides of the rectangular channel. Fluid flow in the fuel cell channel is indeed laminar (Re < 2000), so the friction factor can be expressed as:

$$f = \frac{c}{Re} \tag{5}$$

where c is the friction coefficient of the rectangular duct and is 62.2 for the present case [30], and Re is the Reynolds number based on the hydraulic diameter and can be expressed as:

$$Re = \frac{\rho V d_h}{\mu} \tag{6}$$

here μ denotes the viscosity.

Using Eqs. (5) and (6) Eq. (4) becomes:

$$\Delta p = \frac{cL\mu V}{2d_h^2} \tag{7}$$

Therefore for the laminar flow the pressure drop is linearly proportional to velocity, i.e., to flow rate.

Table 2
Physical properties and operational parameters for single channel.

Porosity, ε	0.1–0.9
Permeability, K (m^2)	10^{-16}–10^{3}
Density, ρ ($kg\,m^{-3}$)	1.251
Viscosity, μ ($kg\,ms^{-1}$)	1.98×10^{-5}
Operational temperature, T (K)	323
Operational pressure, P (pa)	101325
Flow rate, Q ($m^3\,s^{-1}$)	3.54×10^{-6}
Gas composition	N_2: 100%
Channel length, l (m)	0.11
Channel width, b (m)	0.001
Channel height, a (m)	0.0005

5. Results and discussions

The physical conditions and the operational parameters used in the numerical simulation are listed in Table 2.

5.1. Model validation

The distribution of pressure from the inlet to the outlet of the channel by numerical simulation and its linear fitting is shown in Fig. 4(a). Here, only the channel region is considered, i.e., the channel without the GDL and to do so, the interface between the channel and GDL is considered as a wall. The pressure drops linearly with the channel length except at the entrance region. Fig. 4(b) shows a close-up view of the entrance pressure drop indicated by the dotted rectangular box in Fig. 4(a). Up to a finite distance from the inlet, the pressure drop does not exactly follow the linear profile and over-estimates the linear fitting.

The pressure drop obtained from the numerical simulation and its linear fitting is compared with the experimental as well as

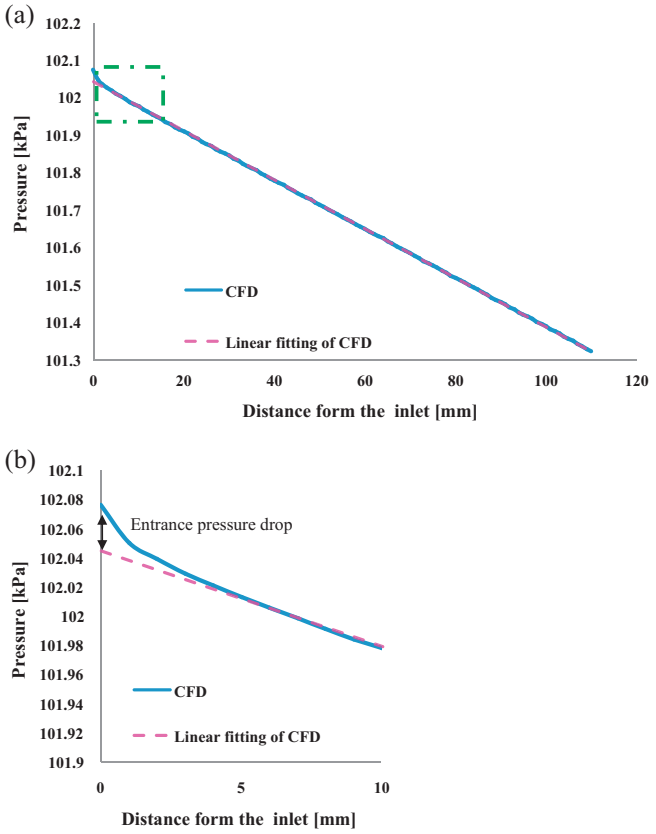

Fig. 4. (a) Pressure distribution in the rectangular channel and (b) close-up view of entrance pressure drop.

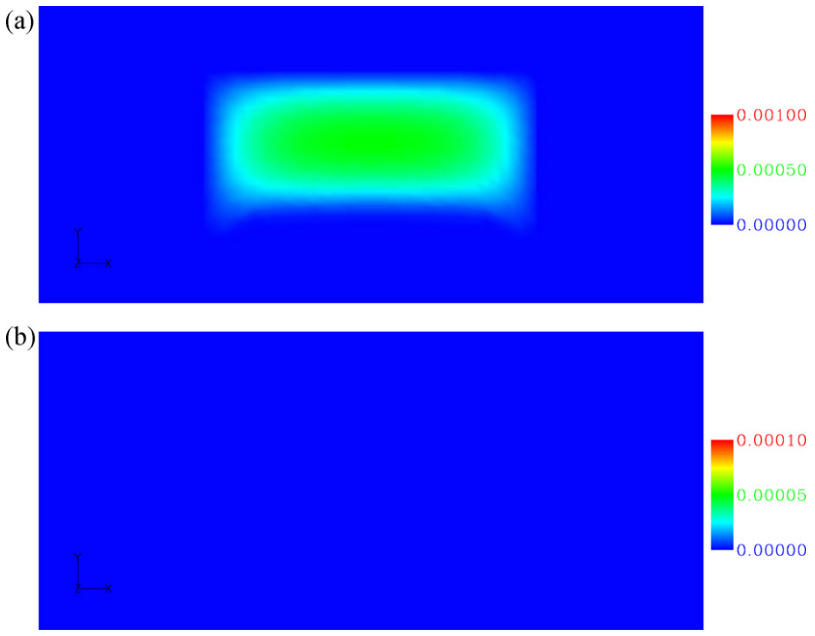

Fig. 5. (a) Residual error of continuity and (b) cross-sectional velocity profile.

theoretical solution. To consider the channel without the GDL case, an experiment was conducted by replacing the GDL with a plastic wall. Eq. (7) was used to find the theoretical solution. The pressure drops obtained by these distinct methods are summarized in Table 3. We see that linear fitting of the numerical results corresponds with the theoretical solution, and an excellent agreement was observed between the numerical and experimental solution. From these results it is also clear that the entrance effect of the pressure drop is included in both the numerical and the experimental results.

Now to find the accuracy of the numerical code, residual error of continuity has been investigated. Fig. 5(a) and (b) shows the spatial variation of residual error of continuity and the cross sectional velocity distribution at the mid cross section of the channel. Contour plot maximum error level is set to 0.1%. From Fig. 5 it is clear that very low level of continuity error is maintained even in the region with high aspect ratio.

5.2. Effect of permeability

The pressure drop for various values of the permeability parameter is shown in Fig. 6. Here the value of the porosity parameter is chosen to be 0.7. We see that the permeability parameter has a very strong effect on the pressure drop. The value of the pressure drop decreases with increasing values of permeability. This can also be interpreted from the Darcy term of momentum equation, which has a direct relation to the permeability. Now from Fig. 6 it is also clear that the representative effect was found for a range of permeability values between 10^{-8} and 10^{-12} m^2. The GDL behaves like an impermeable wall for the values of permeability smaller than 10^{-13} m^2. The value of the pressure drop remained unchanged for permeability values greater than 10^{-7} m^2.

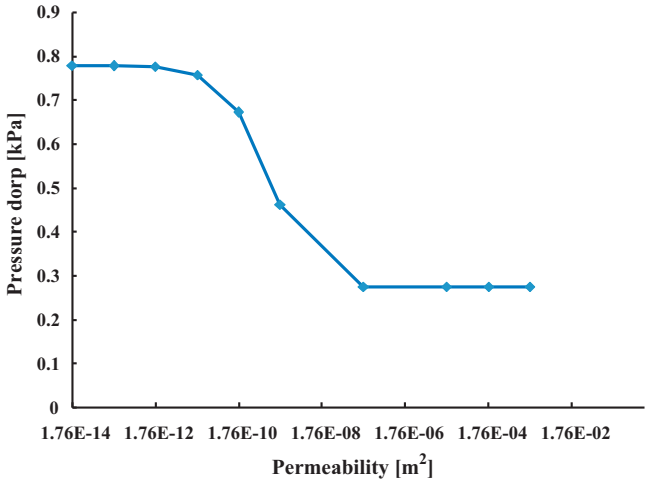

Fig. 6. Pressure drop for a wide range of permeability values.

5.3. Effect of porosity

The pressure drop for different values of the porosity parameter is shown in Fig. 7. Here the permeability value 1.76×10^{-10} m^2 is used for any values of the porosity. We see that the pressure drop increases with the increasing values of porosity, but the effect is not so noticeable.

5.4. Compression and GDL deformation

Table 4 shows the pressure loss obtained by the experimental result with the consideration of 0.1 mm deformation thickness. An analytic solution considering different channel heights (0.5 mm and

Table 3
Comparison of pressure drop obtained by experimental, numerical and analytic method.

	Experimental (kPa)	CFD (kPa)	CFD (Linear fitting) (kPa)	Analytic (kPa)
Without GDL	0.75	0.75	0.72	0.72

Table 4
Pressure drop with and without considering the channel height decrease.

Experimental pressure drop (kPa)	Analytic (a = 0.5 mm) pressure drop (kPa)	Analytic (a = 0.4 mm) pressure drop (kPa)
1.235	0.72	1.288

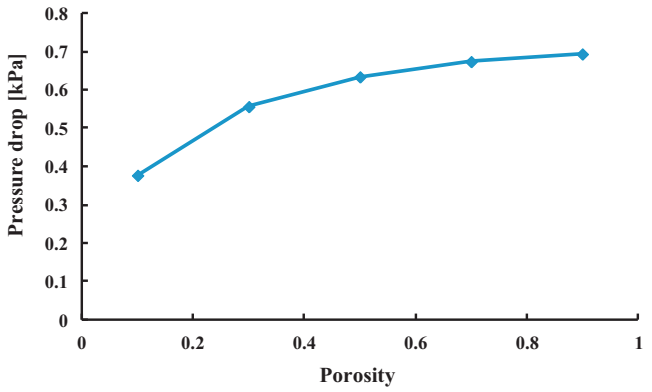

Fig. 7. Pressure drop over porosity.

0.4 mm) is also listed together with the experimental result. Eq. (7) was used for the analytic solution, which is the pressure drop for a rectangular channel with solid walls. The values of the friction coefficient c, for 0.4 mm and 0.5 mm channel heights were 65.47 and 62.2, respectively [30]. We observed that without considering the decrease of the channel height, the analytic solution underestimated the experimental solution for the pressure drop. The flow rate is expressed as: Flow rate = Inlet cross sectional area × Inlet velocity. From the Darcy law we see that pressure drop is linearly proportional to the velocity. So, the lower estimation of the pressure drop derived from the lower estimation of velocity. The flow rate $Q = 3.54 \times 10^{-6}\ m^3 s^{-1}$ remained constant in all cases. Therefore, the velocity becomes higher when we consider that inlet cross sectional area is decreased by the deformation of GDL. Hence, the pressure drop underestimation is attributed to a decrease of the channel height causing GDL intrusion into the channel clamped by the separator land. Thus, the relationship between the GDL deformation and the pressure drop is identified.

With and without applying the clamping pressure, the pressure drop from the inlet to the outlet of the channel was measured and is shown in Fig. 8. The results obtained by the numerical simulation were then compared with the experimental results. The material property of the GDL, i.e., porosity and permeability, used in the experiment is unknown. For this reason taking other parameters as the same we observed several cases and found the values of porosity and permeability at which the same pressure drop as in the experimental result could be obtained without considering the GDL deformation. We found that for the values of porosity = 0.7 and permeability = $2.25 \times 10^{-10}\ m^2$ we could obtain the same pressure drop as in the experimental result of the non-deformed case.

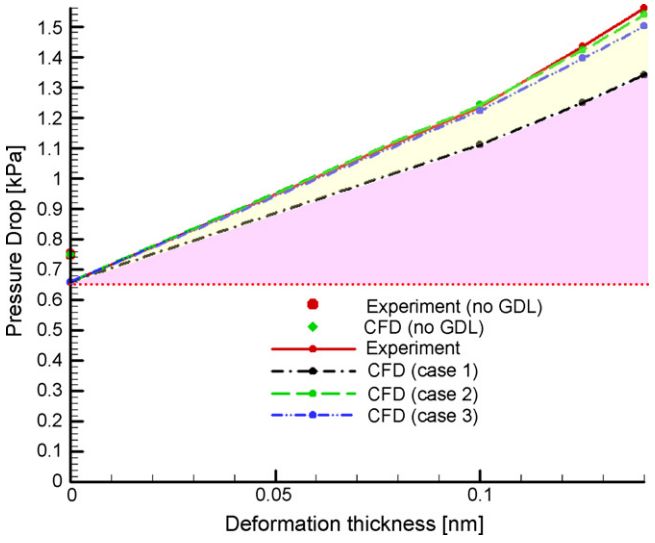

Fig. 8. Comparison of numerical results with different parameters and with experimental results; Case 1: the porosity and permeability of the case with GDL deformation was the same as in the case without deformation, case 2: the permeability was changed but not the porosity and case 3: both the porosity and permeability were changed.

The distance between the two separators, which include anode and cathode GDLs, each with a thickness of 0.3 mm, and the MEA with a thickness of 0.03 mm, was measured. Then 0.24, 0.74 or 1.24 MPa surface pressure was applied and the distance between the two separators in each surface pressure case was measured, which was 0.43, 0.38 and 0.35 mm, respectively. The displacement between the separators after applying the surface pressure distributed evenly to the anode and cathode GDL was considered the deformation thickness. The deformation of the MEA (membrane electrolyte assembly) was neglected due to its very large elastic modulus and very small thickness compared to GDL. The deformation thicknesses for the corresponding cases were 0.1, 0.125 and 0.14 mm. The pressure drop in each deformation case was then measured and is shown in Fig. 8.

In the CFD (computational fluid dynamics) simulation, three distinct cases were considered for each deformation: (1) the porosity and permeability of the case with GDL deformation was the same as in the case without deformation, (2) the permeability was changed but not the porosity and (3) both the porosity and permeability were changed. The pressure drop for each case is shown in Fig. 8. The porosity variation is considered by the following equation (Fluckiger, 2008):

$$\varepsilon = 1 - \frac{\delta_0}{\delta}(1 - \varepsilon_0) \tag{8}$$

where ε_0, δ_0, ε, δ are the uncompressed and compressed porosity and deformation thickness, respectively. The permeability variation is considered by following the experimental results of Nitta et al. [24], where the reduction of permeability was expressed in terms of the deformation thickness. In the numerical solution of case 1 we considered the deformation shape; i.e., the decreased channel thickness was taken into consideration but the change of physical parameters was not considered. From Fig. 8, we see that only considering the deformation shape cannot capture the experimental result. Hence, the change of physical parameters together with the deformation shape was also taken into account in the numerical solutions of case 2 and case 3. We already observed from Figs. 6 and 7 that permeability has a significant effect on the pressure drop but the porosity effect is not so strong. Therefore, the effect of porosity on the pressure drop is indistinguishable. From Fig. 8 we also observed that considering the variation in permeability together with the deformation shape results in good agreement with the experimental result. This result shows the importance of considering the GDL deformation shape along with GDL physical parameter variations in predicting the actual flow phenomena.

5.5. Mechanism of pressure loss

Here we tried to identify the pressure loss mechanism presented in Fig. 8. The horizontal red dotted line indicates the level of pressure drop without consideration of the deformation shape. The shaded region from this horizontal line, indicated by the same parameter, represents the contribution of shape deformation. The shape deformation increases the flow velocity in the channel, and the pressure loss is proportional to velocity. From the black line to green line, the yellow shaded region in Fig. 8 is the contribution of the decrease of permeability, as we already know that the porosity effect is insignificant. We can divide this contribution in two ways: (1) increasing the flow velocity in the channel region (2) frictional drag.

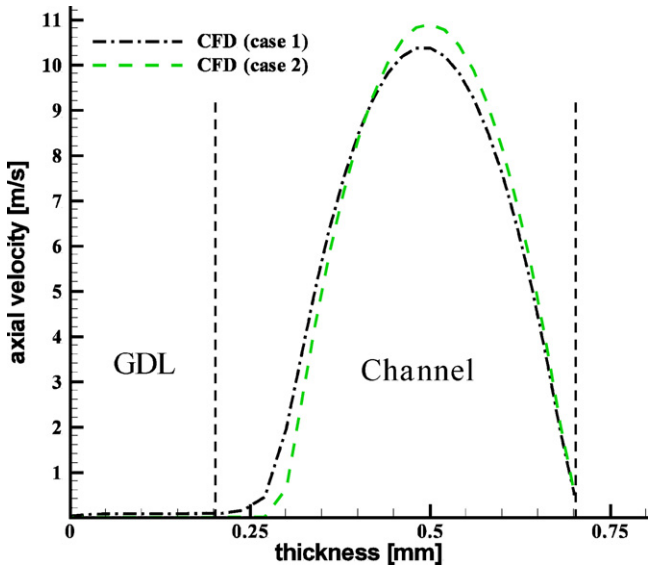

Fig. 9. Velocity profile for case 1 (the porosity and permeability of the case with GDL deformation was the same as in the case without deformation) and case 2 (the permeability was changed but not the porosity).

Fig. 9 represents the axial velocity profile of the middle of the channel and the GDL for the 0.1 mm deformation case. The black line indicates the CFD (same parameter) and the green line indicates the CFD (*K*-change), which is the same as in the legend of Fig. 9. From this figure we see that the axial velocity increases for decreasing values of permeability. The flow rates (or velocity) in the channel region for these two cases are 2.30×10^{-6} and 2.36×10^{-6} $m^3 s^{-1}$ (or 5.47 and 5.62 ms^{-1}). So the decrease of permeability in this case increases the flow rate or velocity in the channel approximately by 3%, and this flow velocity contribute to expanding the pressure loss around 30 Pa, which is approximately 25% of the yellow shaded region. Hence, the remaining 75% is the contribution from the solid matrix drag.

6. Conclusions

The flow behavior in the gas channel and porous GDL of proton exchange membrane fuel cells was investigated by a transient, isothermal three-dimensional numerical simulation. A verification experiment was conducted and data of physical parameters were acquired by mechanical and electrochemical measurements. It has been observed that the permeability parameter has a strong effect on the pressure drop. Also, it is shown that the major effect occurs for permeability values between 10^{-8} and 10^{-12} m^2. The estimation of the pressure drop with and without GDL deformation has been verified by comparing it with the experimental result. The importance of the GDL physical parameter change to estimate the actual flow phenomenon in a real system has been identified. The contribution of the flow rate and the solid matrix drag term on the pressure drop mechanism has been clarified. Moreover, the results indicate that the physical parameter change under the deformed condition can be estimated quantitatively.

Acknowledgment

Financial support of this research by the New Energy and Industrial Technology Development Organization (NEDO), Japan is greatly acknowledged.

References

[1] F. Barbir, H. Gorgun, X. Wang, J. Power Sources 141 (2005) 96–101.
[2] L. Wang, A. Husar, T. Zhou, H. Liu, Int. J. Hydrogen Energy 28 (2003) 1263–1272.
[3] X. Li, I. Sabir, J. Park, J. Power Sources 163 (2007) 933–942.
[4] X. Li, I. Sabir, Int. J. Hydrogen Energy 30 (2005) 359–371.
[5] D.H. Jeon, S. Greenway, S. Shimpalee, J.W. Van Zee, Int. J. Hydrogen Energy 33 (2008) 1052–1066.
[6] M.F. Ferng, A. Su, Int. J. Hydrogen Energy 32 (2007) 4466–4476.
[7] S. Shimpalee, J.W. Van Zee, Int. J. Hydrogen Energy 32 (2007) 842–856.
[8] W. He, G. Lin, T.V. Nguyen, AIChE J. 49 (2003) 3221–3227.
[9] T. Kanezaki, X. Li, J.J. Baschuk, J. Power Sources 162 (2006) 415–425.
[10] J. Park, X. Li, J. Power Sources 163 (2007) 853–863.
[11] E. Passalacqua1, G. Squadrito, F. Lufrano, A. Patti, L. Giorgi, J. Appl. Electrochem. 31 (2001) 449–454.
[12] L.R. Jordan, A.K. Shukla, T. Behrsing, N.R. Avery, B.C. Muddle, M. Forsyth, J. Power Sources 86 (2000) 250–254.
[13] E. Passalacqua, G. Squadrito, F. Lufrano, A. Patti, L. Giorgi, J. Appl. Electrochem. 31 (2001) 449–454.
[14] E. Antolini, R.R. Passos, E.A. Ticianelli, J. Power Sources 109 (2002) 477–482.
[15] J.P. Owejan, T.A. Trabold, D.L. Jacobson, M. Arif, S.G. Kandlikar, Int. J. Hydrogen Energy 32 (2007) 4489–4502.
[16] E.R. Antolini, R. Passos, E.A. Ticianelli, J. Appl. Electrochem. 32 (2002) 383–388.
[17] P. Zhou, C.W. Wu, G.J. Ma, J. Power Sources 159 (2006) 1115–1122.
[18] P. Zhou, C.W. Wu, G.J. Ma, J. Power Sources 163 (2007) 874–881.
[19] P. Zhou, C.W. Wu, J. Power Sources 170 (2007) 93–100.
[20] W.R. Chang, J.J. Hwang, F.B. Weng, S.H. Chan, J. Power Sources 166 (2007) 149–154.
[21] R. Roshandel, B. Farhanieh, E. Saievar-Iranizad, Renew. Energy 30 (2005) 1557–1572.
[22] R. Roshandel, B. Farhanieh, Int. J. Hydrogen Energy 32 (2007) 4424–4437.
[23] V. Gurau, F. Barbir, H. Liu, J. Electrochem. Soc. 147 (2000) 2468–2477.
[24] I. Nitta, T. Hottinen, O. Himanen, M. Mikkola, J. Power Sources 171 (2007) 26–36.
[25] S. Basu, J. Li, C. Wang, J. Power Sources 187 (2009) 431–443.
[26] W. Shi, H. Zhang, E. Kurihara, L.K. Saha, N. Oshima, Proceedings of International Symposium on EcoTopia Science, Nagoya, Japan, 2007.
[27] W. Shi, E. Kurihara, N. Oshima, J. Power Sources 182 (2008) 112–118.
[28] S. Mazumder, C.J. Vernon, J. Electrochem. Soc. 150 (2003) A1503–A1509.
[29] L.K. Saha, E. Kurihara, N. Oshima, J. Fluid Sci. Technol. 5 (2010) 259–269.
[30] F.M. White, Fluid Mechanics, Fifth ed., McGraw-Hill, New York, 2005.